Assessment of RF induced heating of coronary stents in 7T MRI

D. Santoro[1], J. M. Vogt[2], W. Renz[3], J. Gellermann[4], F. Seifert[5], V. Tkachenko[4], J. Schulz-Menger[4], and T. Niendorf[1,4]

[1]Berlin Ultra-High Field Facility (BUFF), Max Delbrück Center for Molecular Medicine (MDC), Berlin, Germany, [2]Department of Physics, Humboldt University Berlin, Berlin, Germany, [3]Siemens Healthcare, Erlangen, Germany, [4]Experimental and Clinical Research Center (ECRC), Charité Campus Berlin Buch, [5]Physikalisch-Technische Bundesanstalt (PTB)

Introduction: The baseline signal-to-noise ratio (SNR) advantage of ultrahigh field MRI holds the promise to enhance, spatial and/or temporal resolution in MRI [1,2,3]. Such improvements would benefit an ever growing set of indications for cardiovascular MR (CMR), including the characterization of ischemic disorders on the myocardial tissue level through mapping microstructures, and parametric imaging [4]. However, intracoronary stents used for treatment of coronary artery disease (CAD) are currently considered to be contra-indications for CMR at 7.0 T. The presence of a metallic implants in combination with RF wave lengths and RF power deposition used at 7.0 T may induce local heating which might cause myocardial tissue damage, influence coagulation or endothelial function. For all these reasons it is essential to carefully assess RF induced heating in coronary stents commonly used in percutaneous coronary intervention. To meet this goal this work examines RF induced heating of coronary stents in agarose phantoms using electromagnetic field (EMF) simulations, fiber optic temperature measurements and MR thermometry at 7.0 T.

Methods: An eight rung highpass circular polarized birdcage RF coil with an inner diameter of 20cm was build to provide RF power which is beyond that of clinical standards. Cylindrical phantoms (V=600ml, d=15cm diameter, 4% agar gel, NaCl-concentration = 3g/l) were setup. A cobalt chromium alloy coronary stent with l=4 cm and d=4 mm (Biotronik, Bülach, CH) was placed into one phantom while the other agarose phantom was used as a control. EMF simulations were performed using the design and geometry of the birdcage coil and of the phantoms (conductivity of 0.77 S/m, the relative permittivity ε_r= 58.24). A FDTD method (CST software, Darmstadt, Germany) was used for EMF and temperature simulation. The proton resonance frequency method (PRF) [5] was used to monitor temperature changes in the phantom experiments. This method derives the temperature changes (ΔT) from the phase difference (Δϕ) of two MR images: $\Delta T = \Delta\phi/(\alpha \cdot TE \cdot \gamma B_0)$ where α is the temperature-dependent chemical shift coefficient (-0.01 ppm/K). A variation of this method has been used, which makes use of the difference of two sets of phase images acquired with different TE [6] to cancel residual phase contributions. For validation, temperature was also measured in four different locations of the phantom using a fiber optics system (Luxtron). RF heating was achieved by repeating the single pulse experiment, with FA=360° (transmit voltage =231V) , TR=1.2ms, Averages=240 (5minutes). After every 5 minutes of RF heating, two 3D-GRE images were acquired (TR=20ms, TEs=4/10ms, FA=20°, FOV=128x128x20cm3, total acquisition time= 72s).

Results: Figs. 1, 2 demonstrate qualitative agreement between simulated and experimental temperature change maps. The simulated map was derived for the stationary solution. Hence it shows much higher ΔT. Fig. 3 shows temperature changes in the presence of a metallic stent in an agarose phantom. For increased accuracy RF irradiation with an absorbed power of 11W resulting in a SAR value of 18.3W/kg was used, which is far beyond the local SAR limits given by the IEC guidelines. Due to the MRI artifact induced by the stent itself, data obtained right at the stent are not considered. Consequently only areas in close proximity to the stent, which showed enough signal in the magnitude image were included. Fig 4 shows the temperature raise in time in the experiment of Fig.3, measured with fiber optics and MR thermometry.

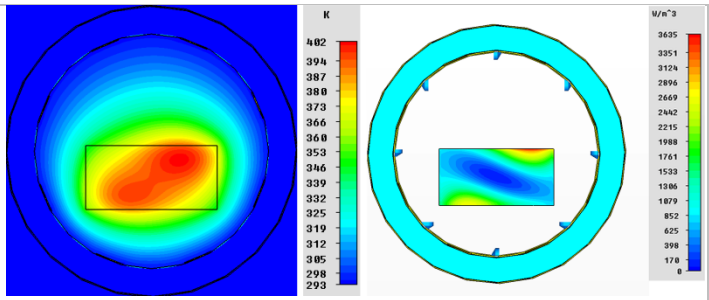

Fig. 1. Simulation of the temperature map (left, in K) and the electromagnetic losses map (right, in W/m^3) in the control virtual phantom induced by RF heating (central axial partition). The stationary solution is shown for the case of a continuous RF irradiation with a power of 50W.

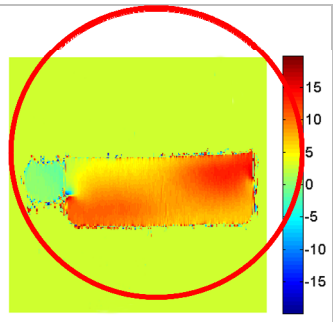

Fig. 2. Experimental temperature changes map (in K) obtained with MR thermometry in the control phantom after 30 min of RF heating (central axial partition). The time averaged absorbed RF power was 11W.

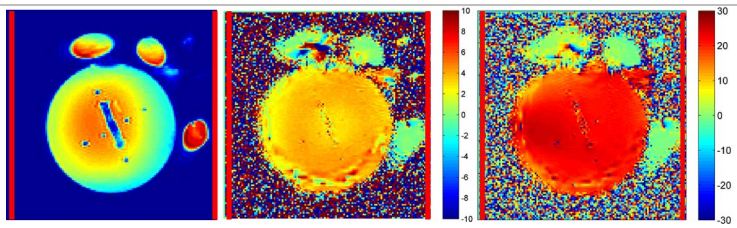

Fig. 3. **Left**: GRE magnitude image of the agarose gel phantom containing the chromium alloy coronary stent in the centre (coronal partition, at the stent position, slightly tilted respect to B_0); also the 6 positions for the fiber optics can be seen (only 4 used). **Centre**: Experimental temperature changes map (in K) obtained with MR thermometry in the same phantom after 10 min of RF heating. **Right**: Same map after 75minutes of RF heating. The time averaged absorbed RF power was 11W. The contour of the coil is given by the red lines.

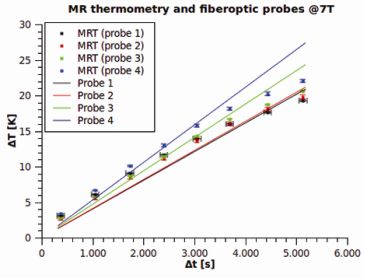

Fig. 4. Temperature time course measured with fiber optics probes and MR thermometry (averaged, near probe locations) for the phantom experiment shown in Fig. 3.

Discussion: Our results show an overall agreement between the simulated temperature maps in a virtual phantom and the temperature maps derived from phantom experiments using MR thermometry. For the chromium alloy coronary stent no extra hot spots were evident in the 3D temperature maps in our setup. Further careful investigations are required before intracoronary stents can be declared to be MR safe in a 7.0 T environment since the presence of metallic stents disturbs the image quality in the close vicinity of the stents.

References:

[1] Hecht EM et al., Magn Reson Imaging Clin N Am 15:449–465, 2007.
[2] Niendorf,T et al., European Radiology (2010-07-31).
[3] von Knobelsdorff-Brenkenhoff et al., European Radiology (2010-07-17).
[4] Mainero et al., Neurology 73:941–948, 2009.
[5] Ishihara Y et al., MRM 34:814–823, 1995.
[6] Gellermann J et al., Int. J. Hyperthermia, 21(6): 497–513, September 2005.